explanation for the increase in pK would be the interaction with a positively charged group of the fragment, e.g., with the side chain of the lysyl residue which is the next neighbor of phosphoaspartate in the sequence.

ACKNOWLEDGMENTS

We thank A. Pfandke for preparing the sarcoplasmic vesicles. We are grateful to the Bruker AG, Karlsruhe, for permitting us to use the AM-400 spectrometer and to Dr. Spraul, Dr. Bermel, and Dr. Kuhn for their help on this instrument.

REFERENCES

Allen, G., & Green, N. M. (1976) *FEBS Lett. 63*, 188-192.
Bastide, F., Meissner, G., Fleischer, S., & Post, R. I. (1973) *J. Biol. Chem. 248*, 8385-8391.
Bock, J. L., & Sheard, B. (1975) *Biochem. Biophys. Res. Commun. 66*, 24-30.
De Meis, L., & Hasselbach, W. (1971) *J. Biol. Chem. 246*, 4759-4763.
Edmondson, D. E., & James, T. L. (1979) *Proc. Natl. Acad. Sci. U.S.A. 76*, 3786-3789.
Fossel, E. T., Post, R. L., O'Hara, D. S., & Smith, T. W. (1981) *Biochemistry 20*, 7215-7219.
Hasselbach, W., & Makinose, M. (1963) *Biochem Z. 339*, 94-111.
James, T. L. (1985) *CRC Crit. Rev. Biochem. 18*, 1-30.
Kalbitzer, H. R., & Rösch, P. (1981) *Org. Magn. Reson. 17*, 88-91.
MacLennan, D. H., Brandl, C. J., Korczak, B., & Green, N. M. (1985) *Nature (London) 316*, 696-700.
Post, R. L., & Kume, S. (1973) *J. Biol. Chem. 248*, 6993-7000.
Sapper, H., Gohl, W., & Lohmann, W. (1980) *Z. Naturforsch., C: Biosci. 35C*, 569-577.
Shull, G. E., Schwartz, A., & Lingrel, J. B. (1985) *Nature (London) 316*, 691-695.
Sontheimer, G. M., Kuhn, W., & Kalbitzer, H. R. (1986) *Biochem. Biophys. Res. Commun. 134*, 1379-1386.
Waki, H., & Hatano, M. (1982) *Polyhedron 1*, 69-75.

Fourier Transform Infrared Investigation of the *Escherichia coli* Methionine Aporepressor†

P. W. Yang and H. H. Mantsch*
National Research Council of Canada, Ottawa, Ontario, Canada K1A 0R6
J. L. R. Arrondo‡
The University of the Basque Country, 48080 Bilbao, Spain
I. Saint-Girons, Y. Guillou, G. N. Cohen, and O. Bârzu
Institut Pasteur, 75724 Paris, France
Received September 15, 1986; Revised Manuscript Received December 4, 1986

ABSTRACT: This study represents the first physicochemical analysis of the recently cloned methionine repressor protein (Met aporepressor) from *Escherichia coli*. Infrared spectrometry was used to investigate the secondary structure and the hydrogen–deuterium exchange behavior of the *E. coli* Met aporepressor. The secondary structure of the native bacterial protein was derived by analysis of the amide I mode. The amide I band contour was found to consist of five major component bands (at 1625, 1639, 1653, 1665, and 1676 cm^{-1}) which reflect the presence of various substructures. The relative areas of these component bands are consistent with a high α-helical content of the peptide chain secondary structure in solution (43%) and a small amount of β-sheet structure (7%). The remaining substructure is assigned to turns (10%) and to unordered (or less ordered) structures (40%). The temperature dependence of the infrared spectra of native Met aporepressor in D_2O medium over the temperature interval 20–80 °C indicates that there are two discrete thermal events: the first thermal event, centered at 42 °C, is associated with the hydrogen–deuterium exchange of the hard-to-exchange α-helical peptide bonds accompanied by a partial denaturation of the protein, while the second event, centered around 50 °C, represents the irreversible thermal denaturation of the protein.

DNA binding proteins, acting specifically as activators or inhibitors of transcription of operons, have been investigated extensively by use of genetic and biochemical approaches (Takeda et al., 1983). The methionine (Met) aporepressor, the polypeptide product of the *MetJ* gene, is a regulatory protein that is required for methionine repression of the methionine regulon (Holloway et al., 1970; Kung et al., 1972; Saint-Girons et al., 1984). Genetic evidence and recent in vitro experiments with the purified Met aporepressor have shown that *S*-adenosylmethionine is the corepressor of the methionine regulon (Greene et al., 1970, 1973; Schoeman et al., 1985; Saint-Girons et al., 1986).

Several properties of the Met aporepressor protein make it attractive for physicochemical studies. It is a small, dimeric protein, each polypeptide chin consisting of 104 amino acid residues, whose primary structure has been deduced from the gene sequence (Saint-Girons et al., 1984). Each monomer binds 1 mol of *S*-adenosylmethionine in an apparently noncooperative manner, suggesting that the two corepressor

† Issued as NRCC No. 25983.
‡ Recipient of a NATO research fellowship.

0006-2960/87/0426-2706$01.50/0 © 1987 American Chemical Society

binding sites are identical and act independently. On the other hand, Met aporepressor does not have a sequence that is highly homologous to the DNA binding domains of regulatory proteins so far investigated (Pabo & Sauer, 1984). It seemed, therefore, important to investigate the physicochemical properties of Met aporepressor in order to understand better the molecular mechanism of the repressor–operator interaction.

As of today, there are virtually no physicochemical, notably spectroscopic, studies of this DNA binding protein. We have therefore performed a detailed Fourier transform infrared (FT-IR) spectrometric investigation of the *Escherichia coli* Met aporepressor, addressing such questions as the protein secondary structure, hydrogen–deuterium exchange, and thermal denaturation.

Infrared spectrometry is one of the earliest experimental methods used for estimating the secondary structure of polypeptides and proteins [for reviews on this subject, see Susi (1972), Parker (1971), and Mendelsohn (1984)]. This structural information is derived from the infrared bands of the conformation-sensitive amide bands, notably from the so-called amide I, amide II, and amide III modes in the infrared spectral region between 1200 and 1700 cm^{-1}. The difficulties with such infrared analysis lie in the fact that these amide bands are broad and the composite band contours consist of a number of individual components. However, the application of new data-reduction methods, in particular, the use of the Fourier deconvolution technique, whereby the broad, overlapping amide bands are narrowed by computational procedures [for a review, see Mantsch et al. (1986)], has allowed more detailed analysis and widened the application of infrared spectrometry to the study of protein structure (Yang, 1983; Susi & Byler, 1983; Yang et al., 1985; Byler & Susi, 1986). The type of information attained by infrared spectroscopic analysis bridges that obtained from X-ray diffraction and circular dichroism analysis; furthermore, the infrared spectra of proteins as solids can be compared with those of the proteins in solution.

Experimental Procedures

Materials. The methionine repressor (Met aporepressor) was obtained from *E. coli* strain GT809 bearing a recombinant plasmid that overproduces this protein. Details regarding the purification of the Met aporepressor protein and purification control by sodium dodecyl sulfate (SDS)–polyacrylamide (12.5%) gel electrophoresis are given elsewhere (Saint-Girons et al., 1986). The sample used in this study was from the same preparation as described above. The bacterial protein was transported from Paris to Ottawa as an ammonium sulfate precipitate; before use it was dialyzed against 10 mM ammonium bicarbonate (pH 7.2) and lyophilized. The lyophilized protein was used for infrared measurements. Aqueous preparation (~4 mM in Met aporepressor) were obtained by dissolving 1 mg of solid protein in 12 μL of 10 mM 4-(2-hydroxyethyl)-1-piperazineethanesulfonic acid (Hepes) buffer (pH 7.2), prepared either with double-distilled water or with D_2O (99.8%).

Infrared Spectra. Infrared spectra of the solid protein were measured from 0.5 mg of lyophilized Met apoprotein as 2 wt % dispersions in high-purity potassium bromide (KBr disk). Aqueous protein samples were measured as liquid films between calcium fluoride windows that were assembled into a demountable liquid cell (Harrick Scientific, Ossining, NY), with 6-μm spacers for samples in H_2O buffer and 12-μm spacers for those in D_2O buffer. A tungsten–copper thermocouple was placed onto the window, and the whole assembly was introduced into a thermostated cell mount. The temperature setting was controlled by a host computer-generated transitor–transistor logic signal at the increment set by the user. Typically, 512 interferograms were signal averaged at an optical retardation of 0.5 cm, triangularly apodized, and Fourier transformed to yield spectra with a spectral resolution of 2 cm^{-1}. The position of the infrared bands was determined with an uncertainty of less than 0.1 cm^{-1} by calculating the center of gravity of each band (Cameron et al., 1982). In order to separate overlapping infrared bands, Fourier deconvolution and Fourier derivation techniques were applied (Mantsch et al., 1986; Moffatt et al., 1986). Curve fitting was performed by standard procedures (Fraser & Suzuki, 1966). Infrared difference spectra were generated by taking the difference between the higher temperature spectrum and the lower temperature spectrum and normalizing with respect to the temperature increment.

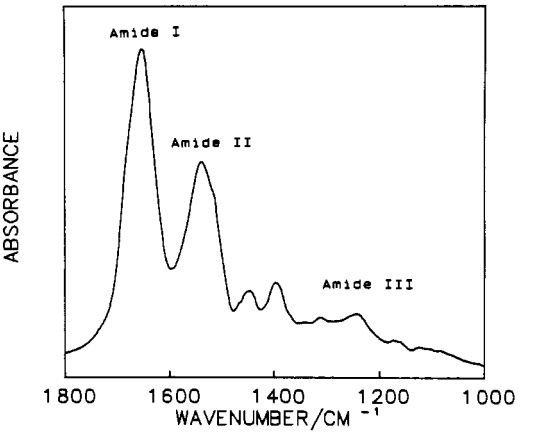

FIGURE 1: Fourier transform infrared spectrum of solid (lyophilized) Met aporepressor.

Results and Discussion

Secondary Structure of Met Aporepressor Protein. The infrared spectrum of solid Met aporepressor is displayed in Figure 1; it is clearly dominated by the strong amide I and amide II bands at 1660 and 1550 cm^{-1}, respectively, while the amide III band around 1300 cm^{-1} is much less prominent. The weaker bands in this spectral region are due to side-chain vibrations.

We have undertaken an analysis of the secondary structure of the Met apoprotein, based on the amide I mode. This spectral region consists of a number of broad overlapping bands that cannot be resolved into individual components by an increase of the instrumental resolution.

Figure 2 shows the amide I band of the solid Met apoprotein in comparison with that of the native protein in aqueous solution. It is immediately evident that there are considerable differences between the infrared spectrum of the protein in the solid state and those in aqueous solution. Furthermore, there are also subtle differences between the spectrum in H_2O and that in D_2O, differences that can be exploited for diagnostic purposes. The center of the amide I band contour is at 1660 cm^{-1} in the solid protein, at 1655 cm^{-1} in H_2O, and at 1650 cm^{-1} in D_2O.

As can be seen from Figure 3A, the amide I and amide II bands of Met aporepressor in D_2O medium are featureless in the original infrared spectra. The center of the band contour of the amide I mode is at 1650 cm^{-1} in the spectrum of the native protein (solid curve) and shifts to 1645 cm^{-1} in the spectrum of the thermally denatured protein (broken curve). Resolution enhancement by Fourier deconvolution [see Mantsch et al. (1986)], as well as by Fourier derivation, an

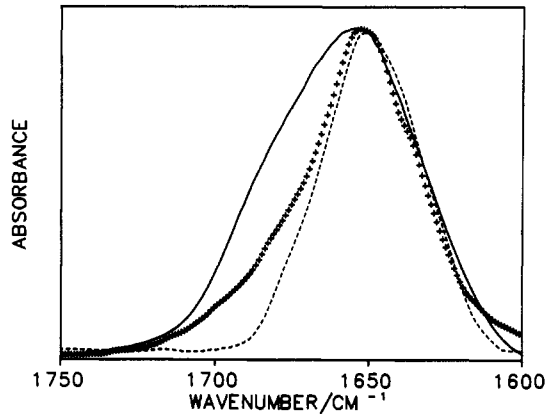

FIGURE 2: Infrared spectra in the region of the amide I band of solid (—) and native Met aporepressor protein in Hepes buffer, pH 7.2, in H_2O (++) and in D_2O (---).

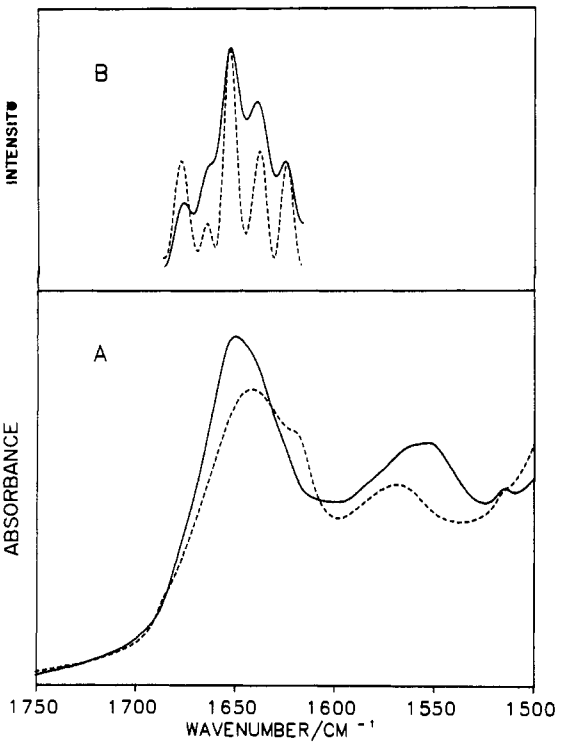

FIGURE 3: (A) Infrared spectra of native (solid curve) and thermally denatured (broken curve) Met aporepressor in D_2O–Hepes buffer, pH 7.2. (B) Infrared spectra of the native protein in the region of the amide I band after resolution enhancement by Fourier deconvolution (solid curve), using a Lorentzian band shape of half-width 20 cm^{-1} and a K value of 2.5 [see Mantsch et al. (1986)], and the same spectra after resolution enhancement by Fourier derivation (broken curve), using a power of 3 and a breakpoint of 0.35 [see Moffatt et al. (1986)].

alternative method to enhance spectral resolution based on the generation of nonintegral derivative band profiles [see Moffatt et al. (1986)], reveals that the complex amide I band contour of the native bacterial protein consists of five individual component bands.

Figure 3B shows the amide I band contour of native Met apoprotein after Fourier deconvolution (solid curve), which reduces the intrinsic widths of the component bands by a factor of 2.5. Fourier derivation, using a power of 3 and a breakpoint of 0.35, also identifies five component bands for the native protein (broken curve in Figure 3B) that are at the same positions as those found by deconvolution.

Once the number and position of the individual bands are determined, they can be used as input parameters for curve-fitting analysis of the original spectrum (without this knowledge curve fitting would be meaningless, or risky at best). Figure 4A illustrates the results of such a curve-fitting procedure applied to the spectrum of native Met aporepressor. It can be seen that the amide I band contour of the native bacterial protein in D_2O buffer consists of a strong center band at 1653 cm^{-1} and four shoulder bands, two on each side of the 1653-cm^{-1} band. The exact positions of these five bands are given in Table I along with their bandwidths at half-height and their total areas (as integrated intensities), which in turn are related to the population of the corresponding substruc-

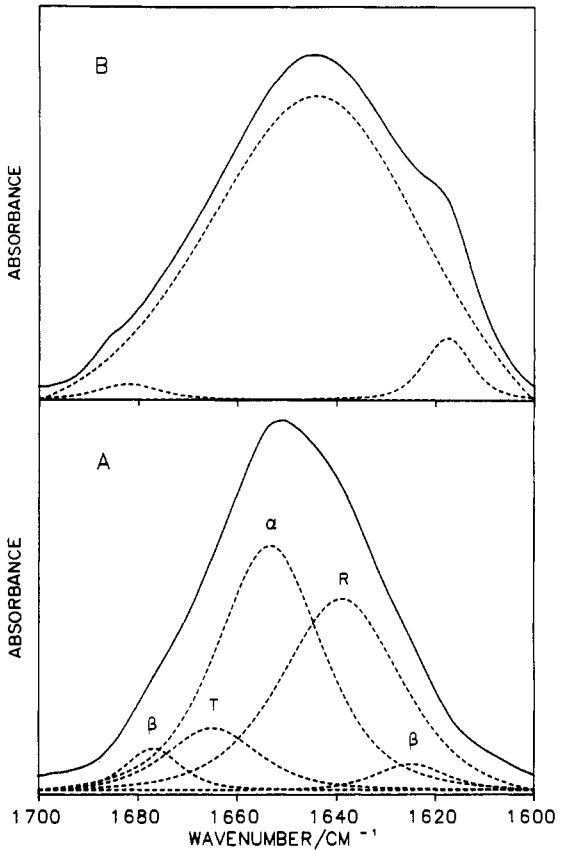

FIGURE 4: (A) Original amide I band contour (solid curve) with the individual component bands (broken curves) for the native Met aporepressor protein in D_2O–Hepes buffer, pH 7.2. The line shapes of the component bands are 0.7 Lorentzian with 0.3 Gaussian. The symbols α, β, T, and R stand for α-helices, β-structures, turns, and random coil, respectively. (B) Amide I band contour of the thermally denatured protein in D_2O buffer (solid curve) with the individual component bands (broken curves).

Table I: Frequencies (ν), Bandwidths at Half-Height ($\Delta\nu_{1/2}$), and Fractional Band Areas (A) of Amide I Band Components of Met Aporepressor Protein[a]

native protein[b]			solid protein[c]		
ν (cm^{-1})	$\Delta\nu_{1/2}$ (cm^{-1})	A (%)	ν (cm^{-1})	$\Delta\nu_{1/2}$ (cm^{-1})	A (%)
1625	17	3	1616	17	2
			1632	27	20
1639	30	40			
			1639	12	1
			1650	22	26
1653	25	43			
			1659	18	10
1665	23	10	1668	21	16
			1678	19	7
1676	14	4			
			1688	27	18

[a] Frequencies and bandwidths are rounded off to the nearest integer. [b] At 30 °C in Hepes–D_2O buffer, pH 7.2. [c] From the IR spectrum of lyophilized Met aporepressor protein.

tures. If the amide I bands are of comparable absorptivities (a reasonable approximation), their integrated intensities are a measure of their relative concentrations. It should be emphasized that the component bands identified by the curve-fitting analysis of the Met apoprotein are essentially the same as those obtained by deconvolution and those found with derivative spectroscopy. The close agreement among these three methods adds confidence to the analysis and suggests that these infrared bands reflect real structural details; curve fitting then provides the added advantage that it allows the relative contributions of the component bands to be estimated.

The component bands derived from the curve-fitting analysis of the amide I mode are best interpreted as reflecting at least four types of substructure in the native protein. The amide I band at 1653 cm^{-1} can be assigned unambiguously to α-helices, while the component bands at 1625 and 1676 cm^{-1} are due to β-structures; in fact, the concomitant appearance of a pair of bands around 1620 and 1680 cm^{-1} has been associated with antiparallel β-sheet structures (Susi et al., 1967).

This leaves two bands to be assigned, one at 1665 cm^{-1}, located between the α-helix band and the high-frequency β-component, and one at 1639 cm^{-1}, placed between the α-helix band and the low-frequency β-component. The 1665-cm^{-1} band is most likely due to turns, as bands around 1665 cm^{-1} have been assigned to turns (Susi & Byler, 1983) as well as to α-type helical structures with distorted hydrogen bonding (Krimm & Dwivedi, 1982). The band at 1639 cm^{-1} requires special attention. While it might reflect the presence of structures intermediate between helices and sheets, in the spectra recorded in H_2O medium this band is not evident as it heavily overlaps the band at 1653 cm^{-1}. Therefore, we prefer to assign it to unordered (or less ordered) peptide segments in which the amide NH group has been replaced by ND groups. Thus, the H → D exchange of the unordered segments (which is accompanied by a downshift in frequency), without the exchange in the ordered α-helices, helps to separate the infrared bands due to the two peptide populations. However, as pointed out by one of the reviewers, the position of the band at 1639 cm^{-1} is also compatible with amide I bands observed for β-structures. We have therefore increased the resolution enhancement close to the limit of the signal-to-noise ratio (data not shown); this splits the 1639-cm^{-1} band into a major component at 1642 cm^{-1} and a minor component at 1638 cm^{-1}. The frequency of the 1642-cm^{-1} band is quite characteristic of disordered proteins in D_2O solution (Byler & Susi, 1986).

From the integrated intensity of these bands, the fractional percentage of α-helical structure in the native protein is 43% (see Table I). The sum of the integrated areas of the β-bands taken as a fraction of the total amide I band area (which should be closely related to the β-content of Met aporepressor) is relatively small, i.e., 7%. The fraction of unordered (or less ordered) protein accounts for 40% of native Met aporepressor. It should be mentioned here that the broad band at 1639 cm^{-1} may also contain a given amount of β-substructures, a fact that could increase the β-content of Met aporepressor. The remaining 10% is assigned to turns.

Though these assignments do not depend on any transferred secondary structure values from model homopolypeptides or on statistical correlations, they are tentative and should eventually be confirmed by X-ray analysis.

We have also analyzed the amide I band of solid Met aporepressor for substructure, insofar as one can talk about the secondary structure of a lyophilized solid protein. From the band contour in the spectrum of the solid protein in Figure 2, one would expect component bands at higher frequencies

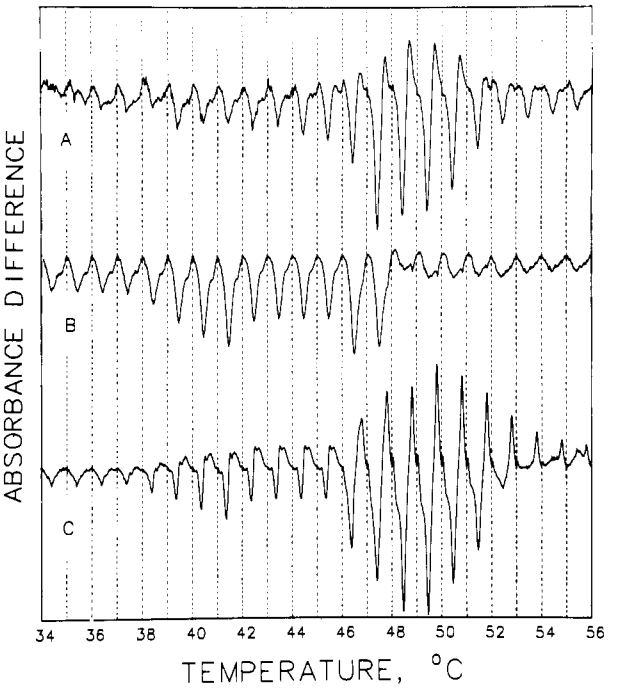

FIGURE 5: Normalized infrared difference spectra at indicated temperatures, obtained from the amide II band of Met aporepressor in H_2O buffer (A), from the amide II band in D_2O buffer (B), and from the amide I band in D_2O buffer (C). The frequency domain illustrated for the difference spectra in (A) and (B) is 1500–1600 cm^{-1} and in (C) is 1600–1700 cm^{-1}.

compared to those in solution (H_2O or D_2O). Resolution enhancement reveals eight component bands in the 1600–1700-cm^{-1} region of the spectrum of solid Met aporepressor. The positions, widths, and integrated intensities of these bands are given in Table I; it is evident that they do not provide a perfect match with the data obtained from the native Met aporepressor. If both bands in the solid protein at 1650 and 1659 cm^{-1} are assigned to α-helices, the sum of their integrated areas leads to an α-helix content of only 36%. On the other hand, in the solid protein there seems to be a much higher content of β-like structures and turns, as judged from the intensity of the bands at 1632, 1668, 1678, and 1688 cm^{-1}.

Temperature-Induced Hydrogen–Deuterium Exchange and Thermal Denaturation of Met Aporepressor Protein. In homopolypeptides and randomly coiled proteins first-order rate constants apply to the hydrogen–deuterium exchange in the C═O···H—N bonding of the peptide backbone. However, there is ample evidence that for protein domains that are in an α-helix the H → D exchange is very slow under ambient conditions; the percentage of hard-to-exchange peptide hydrogens is often taken as an index of the α-helical content of the protein. On the other hand, upon an increase in temperature eventually all peptide bonds can be exchanged.

We have therefore performed a thermal stability study of the Met apoprotein in aqueous solution (H_2O as well D_2O). Figure 5 shows three series of infrared difference spectra obtained from the absorption spectra of the aqueous protein (4 mM in Hepes buffer, pH 7.2); identical results were obtained with 0.4 mM protein. The selected spectral regions are the region of the amide II band in H_2O buffer (Figure 5A), the amide II band in D_2O buffer (Figure 5B), and the amide I band in D_2O buffer (Figure 5C). These infrared difference spectra were obtained in steps of 1 °C and reflect the changes in the nature of these vibration bands (i.e., the structure of the peptide bonds) as a function of temperature. There are two temperature domains that exhibit changes with temper-

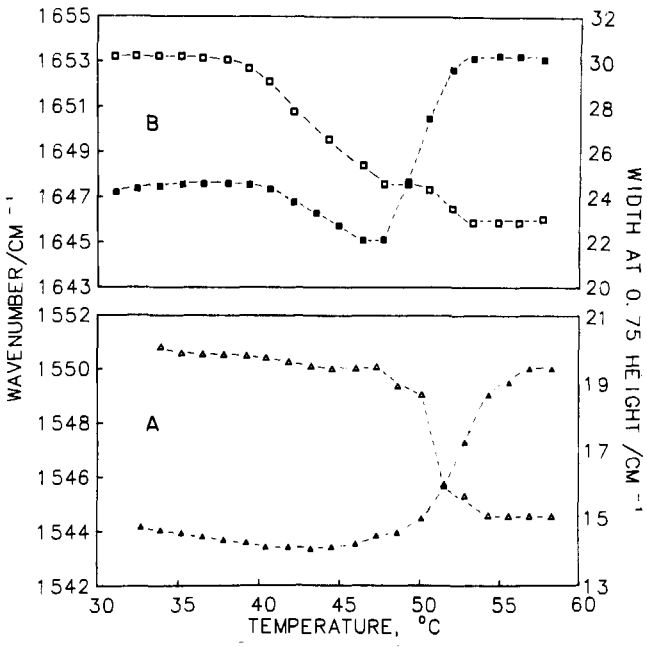

FIGURE 6: Temperature dependence of indicated infrared spectral parameters, derived from the amide II band of Met aporepressor protein in H_2O buffer (A) and from the amide I band in D_2O buffer (B). Open symbols and the left-hand scale represent frequencies, and closed symbols and the right-hand scale are bandwidths.

ature, one between 38 and 46 °C (centered at 42 °C) and another between 46 and 53 °C (centered at 50 °C). Below 38 °C and above 53 °C the changes in the infrared difference spectra are negligible.

The nature of the structural changes reflected by the spectral parameter represented in Figure 5A identifies the high-temperature event as the thermal denaturation of the protein in H_2O medium. These infrared difference spectra represent a typical "melting" of the C=O···H—N peptidic hydrogen bonds. Upon denaturation, the exposed C=O and H—N moieties engage in nonspecific hydrogen bonding to water (H_2O), which leads to a low-frequency shift and a considerable broadening of the amide II band. This is illustrated in Figure 6A, which shows that the position of the amide II band decreases abruptly at temperatures around 50 °C (open triangles) while the width of this band increases considerably between 46 and 53 °C (solid triangles).

The spectral parameter represented in Figure 5B, which shows changes in the low-temperature domain, indicates that this temperature event represents the H → D exchange of the hard-to-exchange α-helix peptides (Parker, 1971). After complete H → D exchange of all peptide NH groups, the amide II band shifts out of this spectral range and there are no further spectral changes upon thermal denaturation.

The spectral parameter illustrated in Figure 5C, which shows changes at both temperature domains, can be used to rationalize the temperature-induced changes in the spectra of the amide I band of Met apoprotein in D_2O medium. As is shown in Figure 6B, at the first thermal event the α-helix band shifts from 1653 to 1648 cm^{-1} (open symbols), while at the second thermal event there is a further small shift in the position of this band, accompanied by a considerable increase in bandwidth (Figure 6B, solid symbols). The decrease of the amide I frequency from 1653 to 1648 cm^{-1} at the first thermal event between 38 and 46 °C suggests that the H → D exchange of the hard-to-exchange α-helices induces a partial denaturation of the native protein, followed by the main melting of the protein at the second thermal event, centered around 50 °C. According to the data in Figure 6, the changes seen at 50 °C in the infrared difference spectrum in Figure 5C reflect primarily the increase in bandwidth due to the melting of the C=O···D—N hydrogen bands.

The band contour of the amide I mode in the thermally denatured Met apoprotein in D_2O medium is shown in Figure 3B. An inspection of this band contour clearly shows a strong band centered at 1645 cm^{-1} and two weak shoulder bands at 1617 and 1682 cm^{-1}. The spectrum of the denatured protein (solid curve) can be easily curve fitted by using these band positions (broken curves). The frequency of the broad band at 1645 cm^{-1} ($\Delta\nu_{1/2}$ = 56 cm^{-1}) is in excellent agreement with those from previous studies of disordered proteins in D_2O solution (Byler & Susi, 1986), while the weak and narrow bands at 1617 ($\Delta\nu_{1/2}$ = 11 cm^{-1}) and 1682 cm^{-1} ($\Delta\nu_{1/2}$ = 15 cm^{-1}) are characteristic of thermally denatured proteins in D_2O medium (unpublished results from this laboratory).

CONCLUSIONS

This investigation illustrates the usefulness of infrared spectrometry for the study of the secondary structure of proteins in solution. The application of new data-reduction methods has allowed us to decompose the complex amide I band contour in the infrared spectrum of the native Met aporepressor protein from *E. coli* into the underlying components and to correlate the individual component bands with a given substructure. The results of this analysis indicate that the predominant form of the peptide chain secondary structure is the α-helix (43%). The other substructures are interpreted as representing β-sheets (7%), turns (10%), and unordered (or less ordered) structures (40%).

Evidently, the description of the secondary structure of Met aporepressor, as well as that of other proteins, in terms of only α-helices, β-structures, turns, and unordered peptide segments is an oversimplification, as one has to expect to deal with substructures or intermediate structures. Furthermore, difficulties arise in extending the correlations derived from homopolypeptides to problems of protein structure, as the group theoretical arguments used to explain the vibrational spectra of model systems [e.g., Miyazawa and Blout (1961) and Krimm and Abe (1972)] may not be applicable to complex globular proteins. The short lengths of ordered segments in the latter, as well as the presence of different side chains, will in principle remove all symmetry and destroy the inter- and intrachain coupling. Thus, these segments may have a range of hydrogen-bonded distances and angles for the peptide groups rather than the fixed values in homopolypeptides. This is expected to be reflected in a complex pattern of infrared bands associated with the stretching vibration of the peptidic carbonyl group (i.e., the amide I mode), and it is gratifying to see that the application of judicious resolution-enhancement techniques allows one to decompose the featureless contour of this highly diagnostic vibrational mode into a number of C=O stretching bands that can be associated with a given secondary structure or substructure.

ACKNOWLEDGMENTS

We thank Drs. H. Casal, W. Surewicz, and R. N. Jones for a critical reading of the manuscript.

REFERENCES

Byler, D. M., & Susi, H. (1986) *Biopolymers 25*, 469–487.
Cameron, D. G., Kauppinen, J. K., Moffatt, D. J., & Mantsch, H. H. (1982) *Appl. Spectrosc. 36*, 245–250.
Fraser, R. D. B., & Suzuki, E. (1966) *Anal. Chem. 38*, 1770–1773.

Greene, R. C., Su, C. H., & Holloway, C. T. (1970) *Biochem. Biophys. Res. Commun. 38*, 1120–1126.
Greene, R. C., Hunter, J. S. V., & Coch, E. H. (1973) *J. Bacteriol. 115*, 56–67.
Holloway, C. T., Greene, R. C., & Su, C. H. (1970) *J. Bacteriol. 104*, 734–747.
Krimm, S., & Abe, Y. (1972) *Proc. Natl. Acad. Sci. U.S.A. 69*, 2788–2792.
Krimm, S., & Dwivedi, A. M. (1982) *Science (Washington, D.C.) 216*, 407–408.
Kung, H.-F., Spears, C., Greene, R. C., & Weissbach, H. (1972) *Arch. Biochem. Biophys. 150*, 23–31.
Mantsch, H. H., Casal, H. L., & Jones, R. N. (1986) in *Spectroscopy of Biological Systems* (Clark, R. J. H., & Hester, R. E., Eds.) pp 1–46, Wiley, Chichester, U.K.
Mendelsohn, R. (1984) *Tech. Life Sci., B1/I Suppl.: Protein Enzyme Biochem. BS110*, 1–37.
Miyazawa, T., & Blout, E. R. (1961) *J. Am. Chem. Soc. 83*, 712–719.
Moffatt, D. G., Kauppinen, J. K., Cameron, D. G., Mantsch, H. H., & Jones, R. N. (1986) *Computer Programs for Infrared Spectrophotometry*, NRC Bulletin No. 18, pp 1–111, National Research Council of Canada, Ottawa, Canada.
Pabo, C. O., & Sauer, R. T. (1984) *Annu. Rev. Biochem. 53*, 293–321.
Parker, F. S. (1971) in *Applications of Infrared Spectroscopy in Biochemistry, Biology and Medicine*, pp 232–270, Plenum, New York.
Saint-Girons, I., Duchange, N., Cohen, G. N., & Zakin, M. M. (1984) *J. Biol. Chem. 259*, 14282–14285.
Saint-Girons, I., Belfaiza, J., Guillou, Y., Perrin, D., Guiso, N., Bârzu, O., & Cohen, G. N. (1986) *J. Biol. Chem. 261*, 10936–10940.
Schoeman, R., Redfield, B., Coleman, T., Greene, R. C., Brot, N., & Weissbach, H. (1985) *Proc. Natl. Acad. Sci. U.S.A. 82*, 3601–3605.
Susi, H. (1972) *Methods Enzymol. 26*, 455–472.
Susi, H., & Byler, D. M. (1983) *Biochem. Biophys. Res. Commun. 115*, 391–397.
Susi, H., Timasheff, N., & Stevens, L. (1967) *J. Biol. Chem. 242*, 5460–5466.
Takeda, Y., Ohlendorf, D. H., Anderson, W. F., & Matthews, B. W. (1983) *Science (Washington, D.C.) 221*, 1020–1026.
Yang, P. W. (1983) Ph.D. Thesis, Department of Chemistry, Ohio University, Athens, OH.
Yang, P. W., Griffiths, P. R., Byler, D. M., & Susi, H. (1985) *Appl. Spectrosc. 39*, 282–287.

Internal Motion and Electron Transfer in Proteins: A Picosecond Fluorescence Study of Three Homologous Azurins†

Jacob W. Petrich,‡,§ James W. Longworth,‖ and Graham R. Fleming*,‡,⊥
Department of Chemistry and James Franck Institute, The University of Chicago, Chicago, Illinois 60637, and Department of Physics, Illinois Institute of Technology, Chicago, Illinois 60616
Received March 21, 1986; Revised Manuscript Received January 8, 1987

ABSTRACT: We have carried out a picosecond fluorescence study of holo- and apoazurins of *Pseudomonas aeruginosa* (azurin Pae), *Alcaligenes faecilis* (azurin Afe), and *Alcaligenes denitrificans* (azurin Ade). Azurin Pae contains a single, buried tryptophyl residue; azurin Afe, a single surface tryptophyl residue; and azurin Ade, tryptophyl residues in both environments. From anisotropy measurements we conclude that the interiors of azurins Pae and Ade are not mobile enough to enable motion of the indole ring on a nanosecond time scale. The exposed tryptophans in azurins Afe and Ade show considerable mobility on a few hundred picosecond time scale. The quenching of tryptophan fluorescence observed in the holoproteins is interpreted in terms of electron transfer from excited-state tryptophan to Cu(II). The observed rates are near the maximum predicted by Marcus theory for the separation of donor and acceptor. The involvement of protein matrix and donor mobility for electron transfer is discussed. The two single-tryptophan-containing proteins enable the more complex fluorescence behavior of the two tryptophans of azurin Ade to be understood. The single-exponential fluorescence decay observed for azurin Pae and the nonexponential fluorescence decay observed for azurin Afe are discussed in terms of current models for tryptophan photophysics.

Proteins are dynamic structures, continuously exchanging thermal energy with their surroundings; their constituent atoms are in a state of continuous motion (Cooper, 1984). The goal of relating protein structure and dynamics, and the possible relation of motion to function, has attracted the efforts of both experimentalists (Ringe & Petsko, 1985) and theoreticians (Karplus & McCammon, 1983; McCammon, 1984).

The naturally occurring aromatic amino acid tryptophan has proved to be a useful fluorescence probe of protein structure (Longworth, 1971, 1983; Beecham & Brand, 1985). In particular, the decay of tryptophyl fluorescence anisotropy has indicated the existence of a local mobility in proteins (Hochstrasser & Negus, 1984; Lakowicz et al., 1983; Munro et al., 1979; Scarlata et al., 1984; van Hoek et al., 1983).

In this paper, we present a study of the time-resolved fluorescence spectroscopy of blue-copper bacterial electron-

† J.W.P. was a pharmacological sciences predoctoral trainee (NIGMS, GM-07151) during the major part of this work and completed parts of it while supported by an NSF Industrialized Countries postdoctoral fellowship and an INSERM poste orange. This work was supported by a grant from NSF to G.R.F.; the Evans and Sutherland PS300/VAX 11-750 molecular graphics system was provided by NSF Grant PCM-8304504.
‡ The University of Chicago.
§ Present address: Laboratoire d'Optique Appliquée, Ecole Polytechnique—ENSTA, INSERM U275, 91128 Palaiseau Cedex, France.
‖ Illinois Institute of Technology.
⊥ Camille and Henry Dreyfus Teacher-Scholar.

0006-2960/87/0426-2711$01.50/0 © 1987 American Chemical Society